Original Article

Computed tomography features for differentiating mast cell tumors and soft tissue sarcomas in subcutaneous masses in dogs

Seri Hong[1] Daji Noh[1] Kija Lee[2] Hojung Choi[3] Youngwon Lee[3] Sooyoung Choi[1*]

Abstract

This study aimed to investigate the computed tomography (CT) features of mast cell tumors (MCTs) and soft tissue sarcomas (STSs) in subcutaneous masses of dogs and to identify distinguishing characteristics between these two tumor types. This retrospective, multicenter study included 22 dogs with subcutaneous masses diagnosed as MCTs (n = 11) or STSs (n = 11) via fine needle aspiration or excisional biopsy. The CT features were evaluated based on four categories: location, morphological characteristics (including shape, margin, capsulation, size, and long axis to short axis (L/S) ratio of the lesion), internal parenchymal characteristics (including cavitation, vascularization, mineralization, homogeneity and Hounsfield Unit within the lesion), and tissue surrounding the lesion (including surrounding tissue involvement and fat stranding around the lesion). Capsulation (P = 0.024), L/S ratio (P = 0.019), cavitation (P = 0.004), and homogeneity in the post-contrast phase (P = 0.036) were significantly different between MCTs and STSs. STSs primarily showed capsulation and cavitation within the mass and were inhomogeneous to heterogeneous in the post-contrast phase, whereas MCTs rarely showed these features and had a higher L/S ratio. Other features did not show significant differences between the two types of tumors. This study reveals that CT analysis of capsulation, cavitation, and homogeneity in the post-contrast phase differentiates MCTs and STSs in subcutaneous masses in dogs.

Keywords: computed tomography, dog, mast cell tumor, soft tissue sarcoma, subcutaneous tumor

[1]*Institute of Veterinary Science and College of Veterinary Medicine, Kangwon National University, Chuncheon 24341, Republic of Korea*
[2]*College of Veterinary Medicine, Kyungpook National University, Daegu 41566, Republic of Korea*
[3]*College of Veterinary Medicine, Chungnam National University, Daejeon 34134, Republic of Korea*
***Correspondence**: choisooyoung@kangwon.ac.kr* (S. Choi)
Received May 20, 2025
Accepted August 6, 2025
https://doi.org/10.56808/2985-1130.3868

Introduction

Subcutaneous tumors are frequently encountered in small animals, especially in dogs. Among these, malignant tumors account for 20–40% of all primary subcutaneous tumors in dogs, with mast cell tumors (MCTs) and soft tissue sarcomas (STSs) being the most common types (MacVean *et al*., 1978; Longo *et al*., 2018). MCTs originate from mast cells or their progenitors and commonly occur in the dermis and subsequently extend into the subcutaneous fat or develop within the subcutaneous fat and do not involve the epidermis (Gianni *et al*., 2024). They are the most common malignant skin tumors, accounting for 22% of all skin tumors (Blackwood, 2011; Martins *et al*., 2022; Gianni *et al*., 2024). Surgery is the primary treatment, and avoiding extensive preoperative manipulation and using antihistamines and corticosteroids is recommended to prevent degranulation and when achieving clear surgical margins is difficult owing to extensive edema (Blackwood, 2011; Wouters *et al*., 2022). Chemotherapy is required to treat disseminated, non-resectable, and high-grade tumors or delay or prevent metastatic disease (Blackwood, 2011).

STSs originate from mesenchymal tissues and are most commonly found in the subcutaneous tissue (Bacon, 2011; Bray, 2016). They are also common malignant skin tumors, accounting for approximately 9–15% of all skin tumors (Ehrhart, 2005; Dennis *et al*., 2011; Bray, 2016). Similar to MCTs, surgery is the primary treatment; however, chemotherapy is less effective as STSs are not chemosensitive, and evidence that chemotherapy extends survival time is insufficient (Bacon, 2011).

Histopathology is the gold standard for diagnosing subcutaneous lesions; however, clinical features and cytology are often used initially to differentiate between malignant and benign tumors (Blackwood, 2011). Typical clinical features of malignant tumors include rapid growth, fixation, invasion into deeper tissues or overlying skin, ulceration, or indistinct margins (Blackwood, 2011). However, MCTs and STSs can mimic clinical features of benign lesions, making initial diagnosis challenging (Blackwood, 2011). Fine needle aspiration (FNA) can diagnose MCTs with high accuracy, but is less effective for STSs (Baker-Gabby *et al*., 2003).

Given the significant differences in prognosis and treatment strategies between these two tumor types, distinguishing them prior to surgery is critical. In addition to clinical features and cytology, imaging diagnostics such as ultrasound and computed tomography (CT) can also be helpful in diagnosis. Several studies have reported on the imaging characteristics of MCTs and subtypes of STSs (Travetti *et al*., 2013; Fukuda *et al*., 2014; Fuerst *et al*., 2017; Spoldi *et al*., 2017; Gianni *et al*., 2024). In addition, a recent study has investigated the imaging features of STSs according to histologic grade (Jeong *et al*., 2025). However, to the best of the author's knowledge, no studies on the differentiation between the two tumor types using CT have been published. Therefore, this study aimed to investigate the CT features of MCTs and STSs among subcutaneous masses and determine distinguishing characteristics between the two tumor types.

Materials and Methods

Case selection: This study had a retrospective, multicenter design. Dogs with subcutaneous mass were collected from Kangwon National University Veterinary Teaching Hospital (Chuncheon, Republic of Korea) from February 2017 to April 2024, The Care Animal Medical Center (Guri, Republic of Korea) from May 2017 to April 2024, and Wonju Sky Animal Medical Center (Wonju, Republic of Korea) from April 2020 to April 2024. Only dogs diagnosed with MCT via FNA or excisional biopsy or STS via excisional biopsy were selected. Dogs that did not undergo CT scans were excluded. The following data were obtained: age, sex, breed, and CT image. Dogs were subsequently classified into MCT and STS groups for analysis.

CT image acquisition: CT scans were conducted using Alexion (Toshiba, Otawara, Japan), Brilliance (Philips, Cleveland, USA), and Revolution ACT (GE Healthcare, Singapore, Singapore) in each of the three institutions with parameters of 1–2 mm slice thickness, 120 kVp, and 50–174 mA. All CT examinations were conducted under general anesthesia, with the dogs positioned in sternal recumbency. All three institutions included pre-contrast and post-contrast phases in the scans. For the post-contrast phase, the ionic iodinated contrast medium, iohexol (Omnipaque™, GE Healthcare, Cork, Ireland), 600–750 mg I/kg IV, was administered via an IV catheter in the cephalic vein. The CT images were reconstructed using a standard kernel for soft tissue and a bone kernel for bony structures in transverse, sagittal, and dorsal planes. The reconstructed images were evaluated using a soft tissue window with a window level of 40 Hounsfield Unit (HU) and a window width of 400 HU and a bone window with a window level of 450 HU and a window width of 1500 HU.

CT analysis: CT images were evaluated using a PACS software program (ViewRex, TechHeim Co., Ltd., Seoul, Republic of Korea). The lesions were evaluated based on four categories: location, morphological characteristics, internal parenchymal characteristics, and tissue surrounding the lesion. All CT features were assessed using post-contrast images, except for homogeneity and HU, which were evaluated in pre- and post-contrast phases, and mineralization, which was assessed using pre-contrast images. All image evaluations were performed by a single observer in a blinded manner, without knowledge of the cytologic or histopathologic diagnosis.

Location: The location of the lesion was classified as being on the head and neck, trunk, or extremities.

Morphological characteristics: The shape of the lesions was classified as plaque, round, oval, or lobular, and if they did not fit any of these categories, they were classified as amorphous. The margin of the lesions was classified as well-defined or ill-defined

(Fig. 1). It was defined as ill-defined if more than 50% of the border between the lesion and the adjacent soft tissue was indistinct. The capsulation of the lesions was classified as present or absent. It was defined as present if there was a sharp distinction between the peripheral border and the internal contents of the lesion. Finally, the maximum and minimum sizes of the lesion in three dimensions and the long axis to short axis (L/S) ratio of the lesion calculated by dividing the maximum size by the minimum size were evaluated (Fig. 2).

Internal parenchymal characteristics: The cavitation of the lesions was classified as present or absent. Cavitation was defined as present if there was a well-defined, low-attenuation area without contrast enhancement within the lesion. The vascularization of the lesion was classified as present or absent. Vascularization was defined as present if vessels were entering directly into the lesions (defined as feeding vessels). The presence of mineralization was classified as present or absent. Mineralization was defined as present if there were areas showing mineral density high attenuation in the pre-contrast phase. Pre-contrast and post-contrast homogeneity of the lesions were classified as homogenous, inhomogeneous, or heterogeneous. Finally, the HU of the lesion, excluding the cavitated area, in the pre-contrast and post-contrast phases was evaluated.

Tissue surrounding lesion: The surrounding tissue involvement was classified as no involvement, contacting, or involvement (Fig. 1). It was defined as "no involvement" if the lesion was not in contact with the surrounding tissue. It was defined as "contacting" if the lesion was in contact with surrounding tissue, but the contrast enhancement of the tissue was normal. It was defined as "involvement" if the lesion was in contact with surrounding tissue and surrounding tissue showed abnormal contrast enhancement compared with normal tissue or if it involved bone with an aggressive bone lesion. Additionally, the fat stranding was classified as present or absent.

Statistical analysis: All statistical analyses were performed using commercial software (SPSS 26.0; IBM SPSS Statistics, New York, USA). The normality of continuous variables (age, size, L/S ratio, and HU) was assessed using the Kolmogorov-Smirnov test. Based on the results of the normality test, age, size, and L/S ratio did not follow a normal distribution and were analyzed using the Mann-Whitney U test. The HU in the pre- and post-contrast phases followed a normal distribution and were analyzed using Student's t-test. All other CT variables were analyzed using Fisher's exact test. Results were considered significant when the *P*-value was less than 0.05.

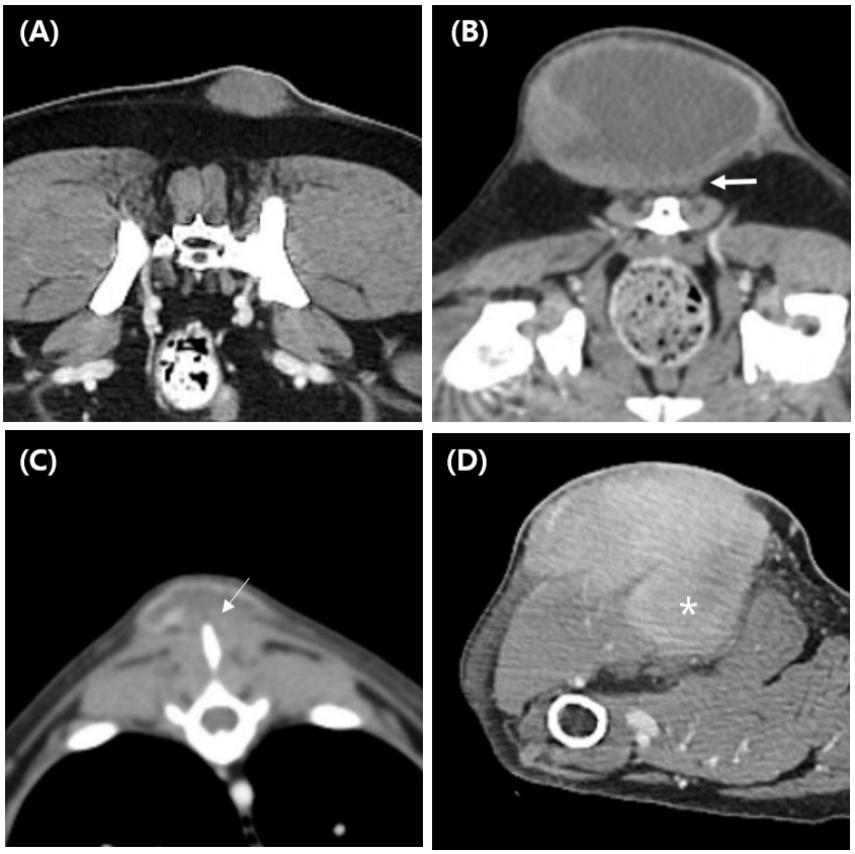

Figure 1 Computed tomography images of subcutaneous masses in dogs showing variations in margin definition and surrounding tissue involvement. (A) Well-defined margin with no surrounding tissue involvement. (B) Well-defined margin in contact with surrounding tissue. (C) Ill-defined margin in contact with surrounding tissue. (D) Ill-defined margin with involvement of surrounding tissue.

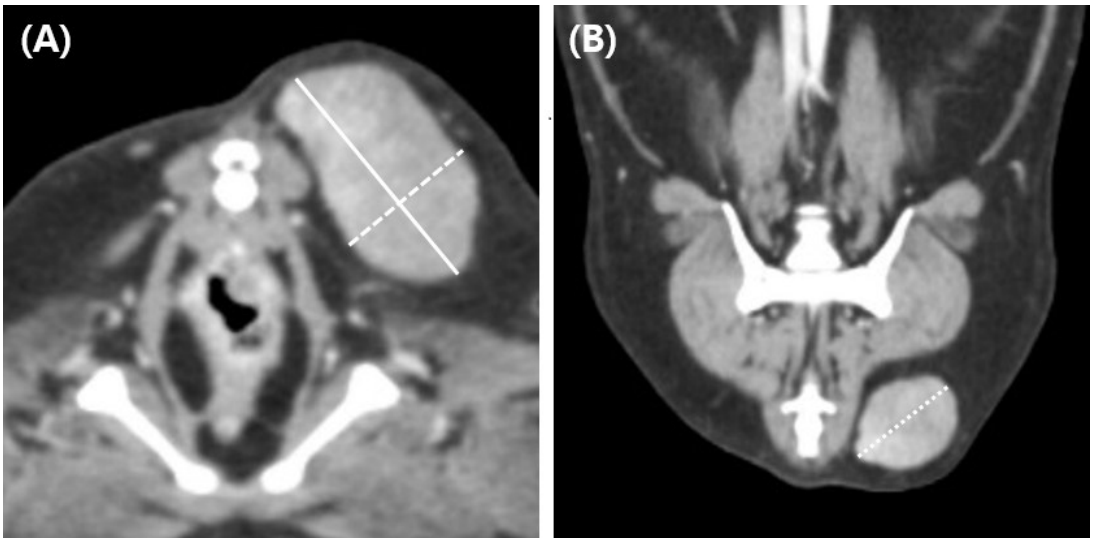

Figure 2 Measurement of long axis to short axis (L/S) ratio in subcutaneous masses. The L/S ratio is calculated by measuring the maximum and minimum sizes in three dimensions (Axis I, Axis II, Axis III) of the mass. (A) Transverse plane image showing the Axis I (Solid line) and Axis II (Dashed line) measurements. (B) Dorsal plane image showing the Axis III (Dotted line) measurement.

Results

Characteristics of cases: A total of 22 dogs were included in this study. The MCT group consisted of 11 dogs, of which six were diagnosed through FNA and five through biopsy. The STS group also comprised 11 dogs, all of which were diagnosed through biopsy. The results of the study are presented in Tables 1–5.

The median age was 7.8 years (range 5–11 years) in the MCT group and 12.1 years (range 4–16 years) in the STS group, with a statistically significant difference between the groups (P = 0.001, Table 1).

CT measurements

Location: The most common location in both groups was the trunk, with no statistically significant difference in location distribution between the groups (P = 0.513, Table 2).

Morphological characteristics: Capsulation was significantly more frequent in the STS group (63.6%) than in the MCT group (9.1%) (P = 0.024, Fig. 3, Table 3). The MCT group had a significantly higher L/S ratio (median 2.9, IQR 2.4–4.0) than the STS group (median 1.8, IQR 1.7–2.2) (P = 0.019). Shape, margin, and maximum and minimum sizes showed no statistically significant differences between the groups (P = 0.416, 1.000, 0.332, and 0.116, respectively).

Internal parenchymal characteristics: Cavitation was significantly more frequent in the STS group (63.6%) than in the MCT group (0%) (P = 0.004, Fig 3, Table 4). The STS group also exhibited a significantly higher degree of heterogeneity in the post-contrast phase than the MCT group (P = 0.036). Vascularization, mineralization, pre-contrast homogeneity, and HU in pre- and post-contrast phases showed no statistically significant differences between the groups (P = 1.000, 1.000, 1.000, 0.461, and 0.087, respectively).

Tissue surrounding the lesion: Surrounding tissue involvement and fat stranding showed no statistically significant differences between the groups (P = 1.000 for both, Table 5).

Table 1 Age, sex, and breed distributions of mast cell tumor and soft tissue sarcoma groups.

		Group	
		Mast cell tumor	**Soft tissue sarcoma**
Age	Median (range)	7.8 (5-11)	12.1 (4-16) *
Sex	Female	3 (27.3%)	1 (9.1%)
	Spayed female	6 (54.5%)	3 (27.3%)
	Male	0 (0%)	2 (18.2%)
	Castrated male	2 (18.2%)	5 (45.5%)
Breed	Labrador Retriever	2 (18.2%)	0 (0%)
	Golden Retriever	2 (18.2%)	1 (9.1%)
	Poodle	2 (18.2%)	1 (9.1%)
	Mix	2 (18.2%)	1 (9.1%)
	Yorkshire Terrier	0 (0%)	2 (18.2%)
	Shih Tzu	1 (9.1%)	1 (9.1%)
	Jindo	1 (9.1%)	1 (9.1%)
	Bichon Frise	1 (9.1%)	0 (0%)
	French Bulldog	0 (0%)	1 (9.1%)
	Schnauzer	0 (0%)	1 (9.1%)
	Maltese	0 (0%)	2 (18.2%)

*The value of soft tissue sarcoma group was significantly higher than that of mast cell tumor group.

Table 2 Location distribution of mast cell tumor and soft tissue sarcoma groups, along with the *P*-value.

		Group		*P*-value
		Mast cell tumor	**Soft tissue sarcoma**	
Location	Head and Neck	2 (18.2%)	3 (27.3%)	0.513
	Trunk	5 (45.5%)	7 (63.6%)	
	Extremities	4 (36.4%)	1 (9.1%)	

Table 3 Comparative analysis of morphological characteristics between groups, along with the *P*-value.

		Group		*P*-value
		Mast cell tumor	**Soft tissue sarcoma**	
Shape	Plaque	0 (0%)	2 (18.2%)	0.416
	Round	1 (9.1%)	3 (27.3%)	
	Oval	7 (63.6%)	5 (45.5%)	
	Lobulated	2 (18.2%)	0 (0%)	
	Amorphous	1 (9.1%)	1 (9.1%)	
Margin	Well-defined	7 (63.6%)	8(72.7%)	1.000
	Ill-defined	4 (36.4%)	3 (27.3%)	
Capsulation (cm)	Present	1 (9.1%)	7 (63.6%)	0.024
	Absent	10 (90.9%)	4 (36.4%)	
Maximum size (cm)	Mean	5.1	5.0	0.332
	Median	2.7	4.6	
	IQR	2.1-5.8	3.6-5.9	
Minimum size	Mean	2.4	2.8	0.116
	Median	1.2	2.6	
	IQR	0.6-2.6	1.7-3.5	
L/S ratio	Mean	3.6	2.1	0.019
	Median	2.9	1.8	
	IQR	2.4-4.0	1.7-2.2	

IQR, interquartile range.

Table 4 Comparative analysis of internal parenchymal characteristics between groups, along with the *P*-value.

		Group		*P*-value
		Mast cell tumor	**Soft tissue sarcoma**	
Cavitation	Present	0 (0%)	7 (63.6%)	0.004
	Absent	11 (100%)	4 (36.4%)	
Vascularization	Present	4 (36.4%)	4 (36.4%)	1.000
	Absent	7 (63.6%)	7 (63.6%)	
Mineralization	Present	0 (0%)	1 (9.1%)	1.000
	Absent	11 (100%)	10 (90.9%)	
Homogeneity in pre-contrast	Hogmogenous	9 (81.8%)	8 (72.7%)	1.000
	Inhomogenous	2 (18.2%)	2 (18.2%)	
	Heterogenous	0 (0%)	1 (9.1%)	
Homogeneity in post-contrast	Hogmogenous	7 (63.6%)	2 (18.2%)	0.036
	Inhomogenous	3 (27.3%)	3 (27.3%)	
	Heterogenous	1 (9.1%)	6 (54.5%)	
HU in pre-contrast	Mean	42.4	38.1	0.461
	Median	40.9	38.0	
	IQR	37.1- 47.2	29.6-41.8	
HU in post-contrast	Mean	87.2	67.1	0.087
	Median	80.8	63.9	
	IQR	70.2-101.7	57.0-75.1	

IQR, interquartile range; HU, Hounsfield Unit.

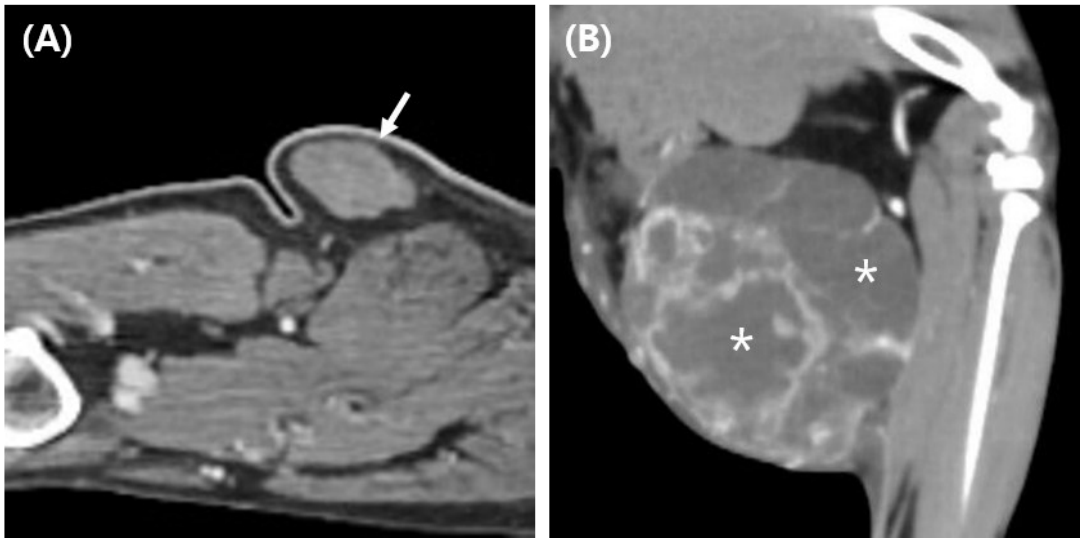

Figure 3 Comparison of computed tomography imaging features between mast cell tumor (MCT) and soft tissue sarcoma (STS). (A) MCT shows no capsulation and cavitation with homogenous enhancement. (B) STS shows capsulation and cavitation with heterogeneous enhancement.

Discussion

This study demonstrates the potential of CT in differentiating between MCTs and STSs. STSs primarily showed capsulation and cavitation within the mass and were usually inhomogeneous to heterogeneous in the post-contrast phase, whereas MCTs rarely showed capsulation and cavitation, were usually homogeneous in the post-contrast phase, and had a higher L/S ratio.

MCTs are not encapsulated (Thamm and Vail, 2012), whereas STSs often possess a pseudo-capsule, which appears as a macroscopic encapsulation despite the histologically poor definition of tumor margins (Bacon, 2011; Wouters *et al*., 2022). This pseudo-capsule is formed by the compression of peritumoral connective tissue, which can contain or be confluent with tumor cells (Torrigiani *et al*., 2019). This characteristic corresponds with the higher capsulation rate in the STS group in this study. The pseudo-capsule, while not a true capsule, can still create a sharp distinction between the tumor and surrounding tissues, making it more likely to be detected on CT and may contribute to the appearance of a capsule on imaging modalities such as CT, supporting our observation of higher capsulation rates in the STS group than in the MCT group.

Compared with the MCT group, the STS group showed significantly more cavitation and were primarily inhomogeneous or heterogeneous enhancement in post-contrast CT images. However, the HU in the post-contrast phase did not show significant differences between the two groups. The reason may be due to the exclusion of cavitated areas during measurement. Therefore, the internal inhomogeneity in the STS group is likely due to the presence of cavitation, supported by the fact that necrosis is considered an important pathological feature in STSs. Necrosis is a critical factor in determining the grade of STS and is a key criterion for assessing the aggressiveness and progression of the tumor (Bray, 2016). In contrast, necrosis is not a primary factor and is generally absent or minimal in MCTs (Thamm and Vail, 2012). However, a direct comparison of the incidence of necrosis between the two has not been well-documented in the literature. In this study, significant differences in cavitation and homogeneity were observed. Previous imaging studies have also reported that STSs are often characterized by heterogeneous or rim, and MCTs typically show homogeneous enhancement (Travetti *et al*., 2013; Fukuda *et al*., 2014; Gianni *et al*., 2024).

STSs tend to infiltrate through fascial planes (Liptak and Forrest, 2012), whereas MCTs exhibit more asymmetrical growth and greater circumferential invasion than deep invasion (Russell *et al*., 2017). This could explain the higher L/S ratio observed in the MCT group. However, some studies do not support this finding. An ultrasound study suggested that STSs tend to be longer than other tumor types, although this difference was not statistically significant (Loh *et al*., 2009). These differing results highlight the need for further study to fully understand the differences in growth patterns between MCTs and STSs and how these might affect imaging features such as the L/S ratio. Therefore, the conclusion about the L/S ratio remains controversial, and further study is necessary.

These tumors are routinely evaluated using CT for surgical planning and staging before surgery (De Nardi *et al*., 2022), and it would be highly beneficial if these two tumors could be differentiated during CT. The significance of this study is based on its identification of specific CT features such as capsulation, cavitation, and homogeneity in the post-contrast phase, which can help accurately differentiate MCTs from STSs preoperatively, thereby contributing to effective clinical decision-making through non-invasive imaging techniques. Furthermore, this study is the first to compare the CT characteristics of these tumors, contributing to a better understanding of veterinary oncology.

However, this study has several limitations. First, the sample size analyzed was relatively small, which may affect the results. The fact that the L/S ratio showed statistical significance and other features did not could be due to the small sample size. Second,

because this was a retrospective, multicenter study, the image settings were not consistently applied across institutions, and there were differences in the timing of post-contrast imaging between centers. Third, in the MCT group, some cases were diagnosed using only cytology, without histopathological examination. Lastly, this study did not analyze tumor grades. While necrosis may be more common in high-grade MCTs and absent or minimal in low-grade STSs, this was not confirmed in our study (Liptak and Forrest, 2012). These limitations may impact the interpretation of the study results, and future studies should aim to resolve these issues.

In conclusion, although there are many overlapping features between MCTs and STSs, CT can help differentiate between the two tumors through characteristics such as capsulation, cavitation, and homogeneity in the post-contrast phase. In particular, in cases of subcutaneous masses in dogs, the presence of capsulation and cavitation with internal inhomogeneity on CT may help increase the likelihood of STSs.

Acknowledgments

This research was supported by the Specialized Graduate Program for Training Wildlife Professionals through the National Institute of Wildlife Disease Control and Prevention, Ministry of Environment (20241104000003125600).

References

Bacon N 2011. Soft tissue sarcomas. In: BSAVA Manual of Canine and Feline Oncology. 3rd ed. Dobson JM, Lascelles BDX (eds). Gloucester: British Small Animal Veterinary Association. pp. 178–190.

Baker-Gabby M, Hunt G and France M 2003. Soft tissue sarcomas and mast cell tumours in dogs; clinical behaviour and response to surgery. Aust Vet J. 81: 732-738.

Blackwood L. 2011. Tumours of the skin and subcutaneous tissues. In: BSAVA Manual of Canine and Feline Oncology. 3rd ed. Dobson JM, Lascelles BDX (eds). Gloucester: British Small Animal Veterinary Association. pp. 130–158.

Bray J 2016. Soft tissue sarcoma in the dog–part 1: a current review. J Small Anim Pract. 57: 510-519.

De Nardi AB, dos Santos Horta R, Fonseca-Alves CE, Paiva FN, Linhares LCM, Firmo BF, Sueiro FAR, Oliveira KD, Lourenço SV, Strefezzi RDF, Brunner CHM, Rangel MMM, Jark PC, Castro JLC, Ubukata R, Batschinski K, Sobral RA, Cruz NO, Nishiya AT, Fernandes SC, Cunha SCS, Gerardi DG, Challoub GSG, Biondi LR, Laufer-Amorim R, Paes PRO, Lavalle GE, Huppes RR, Grandi F, Vasconcellos CHC, dos Anjos DS, Luzo ACM, Matera JM, Vozdova M and Dagli MLZ 2022. Diagnosis, prognosis and treatment of canine cutaneous and subcutaneous mast cell tumors. Cells. 11: 618.

Dennis M, McSporran K, Bacon N, Schulman F, Foster R and Powers B 2011. Prognostic factors for cutaneous and subcutaneous soft tissue sarcomas in dogs. Vet Pathol. 48: 73-84.

Ehrhart N 2005. Soft-tissue sarcomas in dogs: a review. J Am Anim Hosp Assoc. 41: 241-246.

Fuerst JA, Reichle JK, Szabo D, Cohen EB, Biller DS, Goggin JM, Griffin JF IV, Aarsvold S and Emerson SE 2017. Computed tomographic findings in 24 dogs with liposarcoma. Vet Radiol Ultrasound. 58: 23-28.

Fukuda S, Kobayashi T, Robertson ID, Oshima F, Fukazawa E, Nakano Y, Ono S and Thrall DE 2014. Computed tomographic features of canine nonparenchymal hemangiosarcoma. Vet Radiol Ultrasound. 55: 374-379.

Gianni B, Franchi R, Mattolini M, Contiero B, Carozzi G, Nappi L, Cammarota R, Caleri E and Rossi F 2024. CT features of cutaneous and subcutaneous canine mast cell tumors and utility of conventional and indirect lymphography to detect clinically unknown mast cell tumors and to map the sentinel lymph nodes. Vet Radiol Ultrasound. 65: 170-180.

Jeong J, Kim M, Koo J, Joo Y, Yu H, Kim M, Kwak J, Kim J and Eom K. 2025. Computed tomographic features of soft tissue sarcomas in dogs: Association with histologic grade. Vet Radiol Ultrasound. 66: e13478.

Liptak JM, Forrest LJ. 2012. Soft tissue sarcomas. In: Withrow & MacEwen's Small Animal Clinical Oncology. 5th ed. Withrow SJ, Vail DM, Page RL (eds). St Louis, MO: Saunders (Elsevier). pp. 425–454.

Loh Z, Allan G, Nicoll R and Hunt G 2009. Ultrasonographic characteristics of soft tissue tumours in dogs. Aust Vet J. 87: 323-329.

Longo M, Bavcar S, Handel I, Smith S and Liuti T 2018. Real-time elastosonography of lipomatous vs. malignant subcutaneous neoplasms in dogs: preliminary results. Vet Radiol Ultrasound. 59: 198-202.

MacVean D, Monlux A, Anderson P, Silberg Jr S and Roszel J 1978. Frequency of canine and feline tumors in a defined population. Vet Pathol. 15: 700-715.

Martins AL, Canadas-Sousa A, Mesquita JR, Dias-Pereira P, Amorim I and Gärtner F 2022. Retrospective study of canine cutaneous tumors submitted to a diagnostic pathology laboratory in Northern Portugal (2014–2020). Canine Med Genet. 9: 2.

Russell D, Townsend K, Gorman E, Bracha S, Curran K and Milovancev M 2017. Characterizing microscopical invasion patterns in canine mast cell tumours and soft tissue sarcomas. J Comp Pathol. 157: 231-240.

Spoldi E, Schwarz T, Sabattini S, Vignoli M, Cancedda S and Rossi F 2017. Comparisons among computed tomographic features of adipose masses in dogs and cats. Vet Radiol Ultrasound. 58: 29-37.

Thamm DH, Vail DM. 2012. Mast cell tumors. In: Withrow & MacEwen's Small Animal Clinical Oncology. 5th ed. Withrow SJ, Vail DM, Page RL (eds). St Louis, MO: Saunders (Elsevier). pp. 402–424.

Torrigiani F, Pierini A, Lowe R, Simčič P and Lubas G 2019. Soft tissue sarcoma in dogs: A treatment review and a novel approach using

electrochemotherapy in a case series. Vet Comp Oncol. 17: 234-241.

Travetti O, di Giancamillo M, Stefanello D, Ferrari R, Giudice C, Grieco V and Saunders JH 2013. Computed tomography characteristics of fibrosarcoma—a histological subtype of feline injection-site sarcoma. J Feline Med Surg. 15: 488-493.

Wouters EGH, van Nimwegen SA, Ryan S, Kirpensteijn J. 2022. Skin and subcutaneous tumors. In: Veterinary Surgical Oncology. 2nd ed. Kudnig ST, Séguin B (eds). Hoboken, NJ: Wiley-Blackwell. pp. 92–143.